Carbohydrate Polymers 92 (2013) 90–97

Contents lists available at SciVerse ScienceDirect

Carbohydrate Polymers

journal homepage: www.elsevier.com/locate/carbpol

Crystalline structure and thermal property characterization of chitin from Antarctic krill (*Euphausia superba*)

Yanchao Wang, Yaoguang Chang[1], Long Yu, Cuiyu Zhang, Xiaoqi Xu, Yong Xue, Zhaojie Li, Changhu Xue*

College of Food Science and Engineering, Ocean University of China, Qingdao 266003, China

ARTICLE INFO

Article history:
Received 25 June 2012
Received in revised form
27 September 2012
Accepted 29 September 2012
Available online 6 October 2012

Keywords:
Antarctic krill
Chitin
Crystalline structure
Thermal property

ABSTRACT

Antarctic krill (*Euphausia superba*) has been widely studied and extensively recognized as a target for commercial fishing. In this study, Antarctic krill chitin was extracted from defatted Antarctic krill shell, and its crystalline structure and thermal properties were characterized by employing Fourier transform infrared spectroscopy, X-ray diffractometry, scanning electron microscopy, thermogravimetry, and differential scanning calorimetry. Results showed that Antarctic krill chitin corresponded to the α-polymorph, and was composed of small, stable, and uniform microcrystals. The degree of N-deacetylation was 11.28 ± 0.86%. The *d*-spacings of Antarctic krill chitin were 9.78 Å and 4.63 Å at (0 2 0) and (1 1 0) planes. The crystalline sizes were 6.07 nm and 5.16 nm at (0 2 0) and (1 1 0) planes, respectively. The activation energy of the polysaccharide chain decomposition was 123.35 kJ/mol and the glass transition (T_g) of Antarctic krill chitin was 164.96 °C.

1. Introduction

Antarctic krill (*Euphausia superba*) has been widely studied and extensively recognized as a primary prey species in the Antarctic marine ecosystem. Not only does krill play a major role in the food web (Alonzo, Switzer, & Mangel, 2003; Everson, 2000; Mangel & Nicol, 2000; Mauchline & Fisher, 1969; Miller & Hampton, 1989), but it is also attracting increasing interest as a target for commercial fishing (Everson & Goss, 1991; Kawaguchi & Nicol, 2007; Nicol & Endo, 1999). Current estimates suggest that its standing biomass is approximately 342–536 million tons (Atkinson, Siegel, Pakhomov, Jessopp, & Loeb, 2009). Moreover, Antarctic krill is considered to be an abundant and suitable source of aquatic protein and lipid (Mayzaud, Albessard, & Cuzin-Roudy, 1998). Its effective utilization would be beneficial to alleviate the food crisis.

Recently, studies on the utilization of protein and lipid from Antarctic krill have been reported (Gigliotti, Davenport, Beamer, Tou, & Jaczynski, 2011; Wang, Xue, Wang, & Yang, 2011), and Antarctic krill oil was approved to be a novel food ingredient by the European Commission (2009). However, krill shells were considered to be the non-edible constituents and were discarded. Moreover, by analyzing the gross chemical composition of krill shell waste, it has been determined that Antarctic krill is a source of chitin (Naczk, Synowiecki, & Sikorski, 1981). Chitin, a partly deacetylated (1-4)-2-acetamido-2-deoxy-β-D-glucan, found in crustacean shells, has been proven to be a useful bioactive component and polymer material (Muzzarelli et al., 2012). Owing to its outstanding biocompatibility, biodegradability, and bioactivities (Farkas, 1990; Fleet & Phaff, 1981), chitin has been applied in various fields, including functional food, cosmetics, agriculture, medicine, paper industry, immobilization support, and wastewater treatment (Bautista-Baños et al., 2006; Rashidova et al., 2004; Sashiwa & Aiba, 2004; Synowiecki, Sikorski, & Naczk, 1982). Additionally, in recent decades, chitin derivatives have received great attention for their special properties (Muzzarelli, 1988). Given this background, the development of Antarctic krill chitin would provide an effective means to utilize the Antarctic krill shell.

The potential application of chitin is related to its crystalline structure and thermal properties (Rinaudo, 2006; Villetti et al., 2002). The discrepancies in the inter- and intra-molecular hydrogen bindings in the chitin structure result in 3 crystalline forms of natural chitin: α-, β-, and γ-chitin (Cabib, 1981; Cabib, Bowers, Sburlati, & Silverman, 1988). Molecules of α-chitin and β-chitin are respectively aligned in antiparallel and parallel fashions (Blackwell, 1969; Minke & Blackwell, 1978; Rudall, 1963), and γ-chitin is a combination of α-chitin and β-chitin (Rudall & Kenchington, 1973). Different sorts of chitin demonstrate various applications and could

* Corresponding author at: College of Food Science and Engineering, Ocean University of China, No. 5 Yushan Road, Qingdao 266003, China. Tel.: +86 532 82032597; fax: +86 532 82032468.
E-mail addresses: wangyc1219@gmail.com, xuech@ouc.edu.cn (C. Xue).
[1] Contributed equally to this work.

0144-8617/$ – see front matter © 2012 Elsevier Ltd. All rights reserved.
http://dx.doi.org/10.1016/j.carbpol.2012.09.084

be used in different areas. The investigation of crystalline structure and thermal properties of chitin would be beneficial to its more reasonable applications.

In this study, we aimed to elucidate the crystalline structure and thermal properties of Antarctic krill chitin.

2. Experimental

2.1. Materials

Frozen Antarctic krill (*E. superba*) squeezed into blocks was provided by Japan Fisheries Co., Ltd. The frozen krill was lyophilized and its shell was separated for the study.

Two commercial samples of α-chitin extracted from shrimp shells (*Metapenaeus affinis*) and snow crab shells (*Chionoecetes opilio*) were purchased from Haili Bioproduct (Laizhou, China).

Squid (*Illex argentinus*) was purchased from Nanshan Aquatic Products Market (Qingdao, China). The pens were carefully extracted, washed thoroughly with distilled water, and lyophilized. Squid pen chitin was extracted according to the method described previously (Lavall, Assis, & Campana-Filho, 2007) and was used as reference sample of β-chitin (Cortizo, Berghoff, & Alessandrini, 2008).

2.2. Extraction of Antarctic krill chitin

Antarctic krill (*E. superba*) shell was mechanically ground into powder. The powder was first defatted according to the method of Bligh and Dyer (1959). Crude chitin was extracted according to the method of Liang, Chang, Tsai, Lee, and Fu (1997). Briefly, the shell was treated with 1.7 M HCl at an ambient temperature for 6 h and then with 2.5 M NaOH at 75 °C for 1 h. The pigments were decomposed by using 1% potassium permanganate. The purified product was lyophilized.

2.3. Chemical composition analysis

The ash and calcium contents of Antarctic krill chitin were determined according to AOAC (2005). The lipid content was analyzed by the method of Bligh and Dyer (1959). The protein content was indirectly measured by performing amino acid analysis: 300 mg of the sample was hydrolyzed with 6 M HCl for 24 h at 110 °C; the hydrolyzate was dissolved and then analyzed using a Biochrom 30, Ltd. amino acid analyzer (Biochrom, Ltd., Cambridge, UK); the protein content was calculated from the total weight of the composing amino acid. The fluoride content was determined according to a modified fluoride electrode method of Adelung, Buchholz, Culik, and Keck (1987). Simultaneously, the composition of defatted krill shell was analyzed as a reference. Composition contents were all calculated on the basis of dried weight.

2.4. Scanning electron microscopy

Samples were coated with a thin Au layer by using a sputter coater (EIKO IB-3) for conductivity and were scanned using a JSM-840 (JEOL, Ltd., Tokyo, Japan) scanning electron microscope.

2.5. Determination of the degree of N-deacetylation

Values of the degree of N-deacetylation (DD) of krill, crab, shrimp and squid pen chitins were determined by an improved derivative UV method (Wu & Zivanovic, 2008). Briefly, 100 mg of the sample was dissolved in 20 mL 85% H_3PO_4 for 40 min at 60 °C with constant stirring. We then used 1 mL clear solution and diluted it to 100 mL with distilled water. The diluted solution was incubated at 60 °C for 2 h before performing the UV measurement. Standard solutions of GlcNA and GlcN were prepared in 0.85% H_3PO_4 at concentrations of 0, 10, 20, 30, 40, and 50 μg/mL.

The UV spectra were obtained by using a Shimadzu 2550 (Shimadzu, Columbia, USA) double beam UV–vis spectrophotometer under the scan mode in the range of 220–190 nm. UV Probe software (Shimadzu, Columbia, USA) was applied to calculate the first derivative spectra at 203 nm. The calibration curve was generated by plotting the first derivative UV values at 203 nm (H_{203}) as a function of GlcAc and GlcN concentration.

The degree of N-deacetylation was calculated using Eq. (1):

$$\mathrm{DD}\,(\%) = 1 - \frac{(m_1/203.21 \times 100)}{(m_1/203.21 + m_2/161.17)} \quad (1)$$

where m_1 is the mass of acetyl-glucosamine in 1 mL chitin solution, calculated from the calibration curve by the corresponding H_{203}; m_2 is the mass of glucosamine in 1 mL chitin solution, calculated as $m_2 = M - m_1$. The mass of chitin (M) in the 1 mL solution was calculated as: $M = (M_1 \times M_3)/(M_1 + M_2)$, where M_1 is mass of solid chitin sample taken for analysis (100 ± 10 mg); M_2 is mass of 20 mL 85% H_3PO_4; M_3 is mass of 1 mL chitin solution in concentrated H_3PO_4.

2.6. Fourier transform infrared spectroscopy

The Fourier transform infrared (FTIR) spectra were measured over the frequency range 4000–400 cm^{-1} by using 32 scans at a resolution of 4 cm^{-1} by using a model VERTEX70 spectrometer (Bruker Corporation, Karlsruhe, Germany) (Liu et al., 2009). Samples were prepared into 0.25 mm thick KBr pellets (1 mg sample in 100 mg KBr) and were stabilized under controlled humidity before determining the spectra. The curves which mathematically best fitted to the original spectrum were obtained by invoking the Gaussian function (Liu et al., 2010) using OriginPro 8.5 software (Originlab Corporation, Northampton, USA). Intensity of the selected absorption band was determined by the baseline method on the basis of OMNIC software package of the instrument.

Crab, shrimp, and squid pen chitins were measured as reference samples in the same condition.

2.7. X-ray diffraction

The X-ray diffraction (XRD) spectra were obtained with Cu Kα radiation (λ = 1.5406 Å) at 50 kV and 40 mA by using a D8 Advance X-ray diffractometry (Bruker Corporation, Karlsruhe, Germany). A continuous scan was performed using a step size of 0.015° and a step time of 0.2 s. All the data were obtained using the MDI jade software package (Jade 5.0, Materials Data, Inc., Japan) (Hu et al., 2007).

Crystalline size normal to the hkl plane ($D_{\perp hkl}$) was calculated from the full width of peak at the half height of the source curve (FWTH) according to Scherrer's equation (1918) Eq. (2), and d-spacing (d) between atomic layers was determined from the resolved angle 2θ using the Bragg equation (Morton & Hearle, 1975) Eq. (3):

$$D_{\perp hkl} = \frac{K\lambda}{\beta_0 \cos\theta} \quad (2)$$

where K is a constant (indicative of crystallite perfection and was assumed to be 1, λ (Å) is the wave length of incident radiation, β_0 (rad) is the width of the crystalline peak at half height, and θ (°) is the diffraction angle corresponding to the crystalline peak:

$$n\lambda = 2d \sin\theta \quad (3)$$

where n is an integer.

Meanwhile, crab and shrimp chitins were measured as reference samples in the same condition.

2.8. Thermogravimetry and differential scanning calorimetry

Thermogravimetry (TGA) was performed from 20 to 800 °C at a heating rate of 10 °C/min in dynamic (30 mL/min) synthetic air atmosphere using a NETZSCH TG 209F1 analyzer (NETZSCH, Selb, Germany).

Activation energy (E_a) for the thermal degradation of chitin was calculated from TGA curves using the method of Horowitz and Metzger (1963) according to Eq. (4):

$$\mathrm{Ln}\left[\mathrm{Ln}\left(\frac{W_O}{W_T}\right)\right] = \frac{E_a\theta}{RT_{\max}^2} \quad (4)$$

where W_O is the initial weight of the polymer, W_T is the residual weight of the polymer at temperature T, $T_{\max}$ is the temperature for maximum reaction rate, R is the general gas constant, and θ is $(T - T_{\max})$. The activation energies were obtained from the slope $(E_a/RT_{\max}^2)$ of Ln[Ln(W_O/W_T)] vs. θ for the major stage of thermal decomposition.

Differential scanning calorimetry (DSC) was conducted using the NETZSCH DSC 200PC analyzer (NETZSCH, Selb, Germany) according to the method of Kittura, Harish Prashantha, Udaya Sankarb, and Tharanathan (2002). 5 mg of sample was placed into a sealed aluminum cup, and an empty cup was used as the reference. Samples were heated at a constant heating rate of 10 °C/min from 0 up to 200 °C, and then maintained at the isothermal stage for 5 min. After cooling with liquid nitrogen, the second heating program was performed from 20 to 600 °C at a constant heating rate of 10 °C/min again. Indium was used to calibrate the instrument. Data were collected and analyzed using the Proteus software package of the equipment.

The TGA and DSC of crab and shrimp chitins were measured as reference samples in the same condition. Samples were all stabilized under controlled humidity before acquiring the spectra (Kittura et al., 2002).

2.9. Statistical

Each measurement was performed in triplicate ($n = 3$). One-way independent measures analysis of variance (ANOVA) was conducted to determine individual differences between treatments by using PASW Statistics 18.0 (IBM SPSS, Inc., 2009, New York, USA). Post hoc analysis was performed using Tukey's test with a significance level of $P < 0.05$.

3. Results and discussion

3.1. Chitin extraction and chemical composition analysis

White lamellar chitin was obtained from Antarctic krill (*E. superba*) shell after demineralization, deproteinization, and decolorization. The yield of chitin product obtained from defatted krill shell was 27.80 ± 1.48%. Previous studies have shown the yields of chitin from various marine sources, including 20% in the crab (*Portunus pelagicus*) shell, 20% in the shrimp (*Parapenaeopsis stylifera*) shell, and 31% in the squid (*Illex argentinus*) pen (Al Sagheer, Al Sughayer, Muslim, & Elsabee, 2009; Cortizo et al., 2008).

The chemical compositions of Antarctic krill shell and chitin based on dried weight were then determined. In comparison with the original shell, the remaining calcium and protein contents in the chitin product were reduced from 4.97% to 0.03% and from 47.61% to 1.19%, respectively. No lipid was identified in the Antarctic krill chitin, and the ash content was 0.12%.

The fluoride content of krill shell was 3.058 g/kg. The special living environment and diet of Antarctic krill (*E. superba*) leads to high fluoride levels in the krill shell. According to the Allowances (1989), the Daily Adequate Intake of fluoride for adult is 3.1–3.8 mg, and more than 10 mg fluoride daily is harmful to humans. Ingesting high amounts of fluoride in the long term may lead to fluorosis, the symptoms of which include, changes in bone structure and enzyme inhibition (Eagers, 1969). However, no organic or inorganic fluoride was detected in the Antarctic krill chitin, indicating that Antarctic krill chitin obtained in this study could be safely used in food processing.

3.2. SEM analysis

As is shown in Fig. 1A, there exist tightly arranged fibers and flexible macromolecules in the krill shell. According to the studies of Lavall et al. (2007), chitin is a major component of the shell reticular skeleton, and that flexible protein macromolecules irregularly inserted are attached to the chitin backbone, and inorganic components are strongly embedded in chitin gaps. In Fig. 1B, the spaces between the chitin chains seemed to be considerably reduced after the extraction of protein and inorganic components. Meanwhile, the pattern observed before treatment was preserved, suggesting that the native structure of chitin was also preserved.

The tightly arranged structure of Antarctic krill chitin accorded with that of α-chitin extracted from shrimp (*M. affinis*), snow crab (*C. opilio*), or lobster (*Thenus orientalis*) (Al Sagheer et al., 2009; Yen, Yang, & Mau, 2009).

3.3. Degree of N-deacetylation analysis

The first derivative UV method offered a simple and fast measurement of DD value with good accuracy and precision (Muzzarelli & Rocchetti, 1985; Wu & Zivanovic, 2008). Therefore, the first derivative UV method was chosen to determine the DD value in this study.

Results showed that the DD values of Antarctic krill chitin, crab chitin, shrimp chitin, and squid pen chitin were 11.28 ± 0.86%, 19.86 ± 1.69%, 16.87 ± 0.72%, and 10.83 ± 0.67%, respectively.

3.4. Fourier transform infrared spectroscopy analysis

The original FTIR spectrum of Antarctic krill chitin is shown in Fig. 2. All of the typical bands of chitin were present. Bands at 3442 and 3267 cm^{-1} corresponded to O—H and N—H stretching vibration, respectively (Fig. 2A) (Cho, Jang, Park, & Ko, 2000; Hu et al., 2007). A well-resolved and medium intensity band was observed at 3105 cm^{-1} (Fig. 2A). This was recognized as characteristic of secondary amides and thus of α-chitin, being either an overtone of amide I or result of Fermi resonance between the overtone of amide II band and NH stretching band (Rudall, 1963). The splitting band of Antarctic krill chitin spectra at 1660 and 1625 cm^{-1} depended on the hydrogen binding between the C=O groups and one type of the O6—H groups from the glucosamine units (Sikorski, Hori, & Wada, 2009). The above mentioned bands were indicative of α-chitin (Mikkelsen, Engelsena, Hansenb, Larsenc, & Skibsted, 1997). As shown in Fig. 2A, they were all in conformity with those of α-chitin from crab and shrimp, and could hardly be distinguished in the spectrum of β-chitin from squid pen. It can be concluded that Antarctic krill chitin corresponded to the α-polymorph.

In addition, absorption bands at 1560 (amide II NH deformation in the CONH plane), 1416 (CH deformation), 1378 (C—CH_3 amide stretching), 1317 (amide III and)CH_2 wagging), 1157 (COC bridge stretching), 1075 (COC stretching in ring), 1028 (CO stretching), 896 (beta linkage), 708, and 606 cm^{-1} could be also clearly distinguished in the spectrum (Muzzarelli et al., 2007).

Due to the complicated and specific hydrogen bonds generated by the OH and NH groups, the original FTIR spectra of chitin (Fig. 2A) was complex and difficult to distinguish separately. Therefore, mathematical best fit curves applied to the original spectra

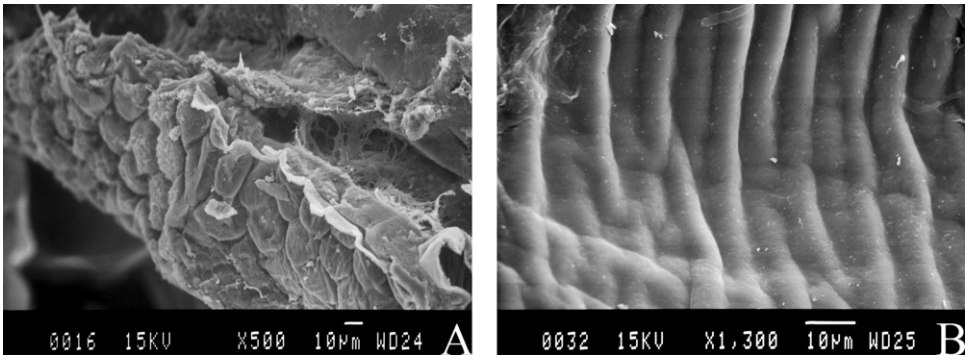

Fig. 1. Scanning electron microscopy (SEM) of Antarctic krill (*E. superba*) shell (A) and Antarctic krill chitin (B).

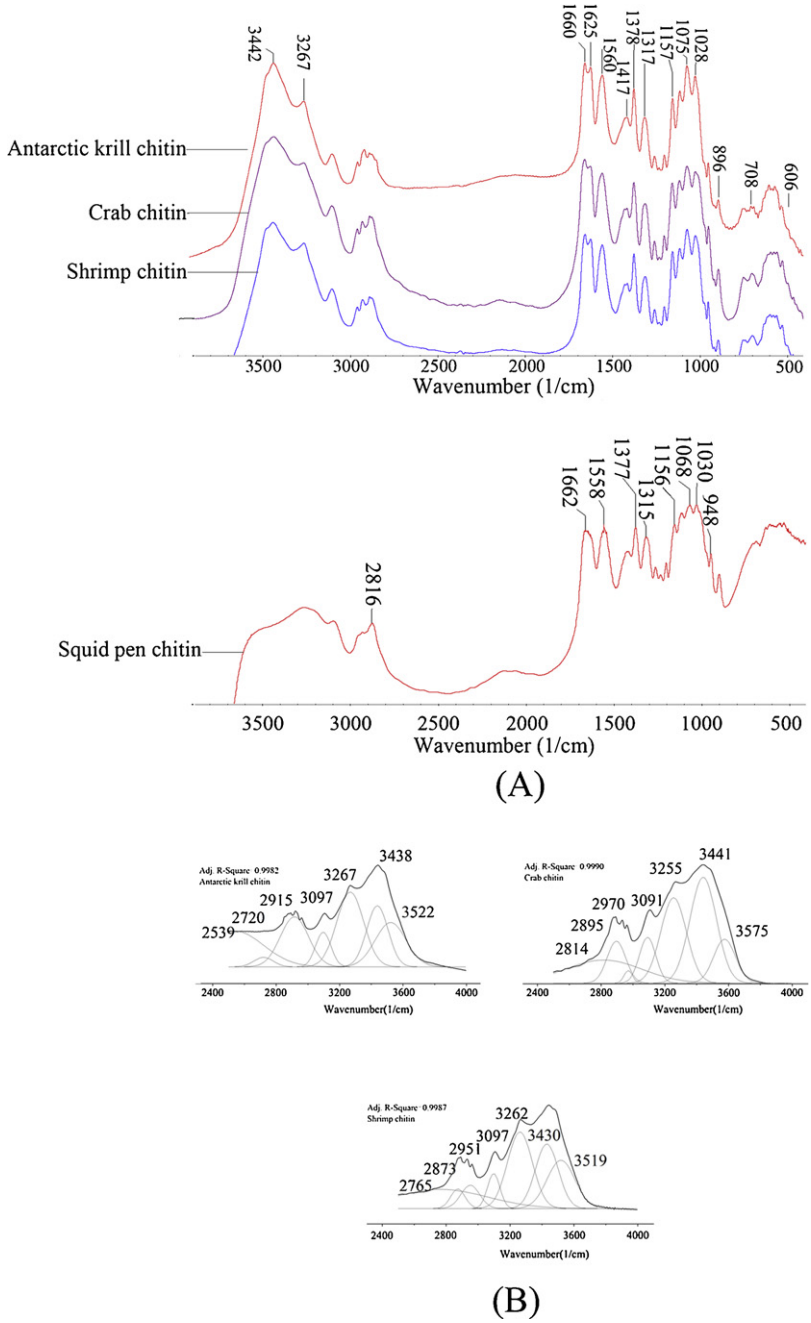

Fig. 2. Original FTIR spectra (A) and their fit curves (B) of Antarctic krill (*E. superba*) chitin, crab (*C. opilio*) chitin, shrimp (*M. affinis*) chitin and squid (*I. argentinus*) pen chitin.

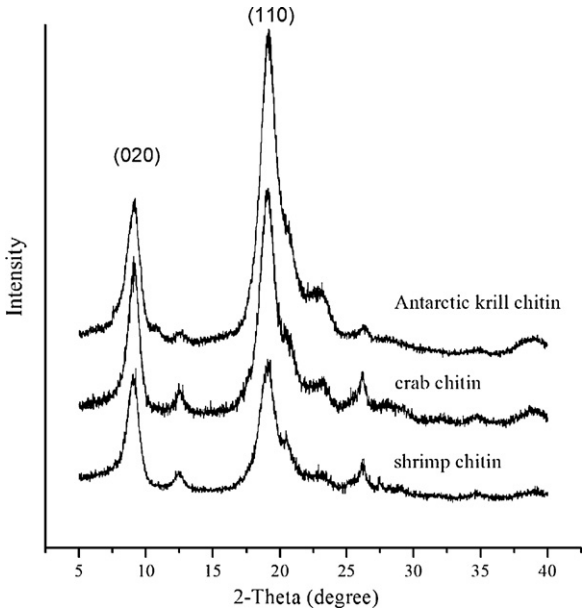

Fig. 3. X-ray diffractometry (XRD) of Antarctic krill (*E. superba*) chitin, crab (*C. opilio*) chitin, and shrimp (*M. affinis*) chitin.

were obtained using the Gaussian function after normalization, and were then separated into each component peak of a symmetric nature associated with $r^2 > 0.99$ (Fig. 2B). According to the previous studies (Liu et al., 2010; Sikorski et al., 2009), the band separations of Antarctic krill chitin at 3438 and 3522 cm^{-1} could be attributed to the stretching of inherent OH and free OH groups, respectively. Meanwhile, the stretching of inherent OH and free OH groups of crab chitin were observed at 3441 and 3575 cm^{-1}. It could be easily found that the band absorbance ratio of free OH groups to inherent OH groups of Antarctic krill chitin is higher than that of crab chitin. This phenomenon suggested that the free OH groups in Antarctic krill chitin might be more than that in crab chitin.

3.5. Crystalline structure analysis

XRD profiles of Antarctic krill chitin and reference α-chitin samples are shown in Fig. 3. X-ray diffraction studies have shown that α-chitin adopted a 2-chain orthorhombic unit cell with the space group $P2_12_12_1$, indicating an antiparallel chain arrangement (Saito, Okano, Chanzy, & Sugiyama, 1995; Sikorski et al., 2009). The reflection peaks at 9.03° and 19.17° in the Antarctic krill chitin diffraction pattern were identified to be diffraction planes (0 2 0) and (1 1 0) of the orthorhombic crystal structure, respectively. Spectrum of Antarctic krill chitin nearly overlapped with the reference α-chitin samples at the above peaks. The spectrum showed that Antarctic krill chitin corresponded to the α-polymorph, which validated the FTIR spectra analysis.

Crystallite sizes and *d*-spacings of krill, crab, and shrimp chitin calculated from the spectra are displayed in Table 1. The *d*-spacings of different chitin samples were nearly the same, while crystallite sizes at (0 2 0) and (1 1 0) planes of Antarctic krill chitin were significantly smaller than those of reference α-chitin samples ($P < 0.05$). The difference between crystals of Antarctic krill chitin and reference α-chitin might result from varied planes and angles of molecular chains in the chitin micro-fibrils, and the inter- or intra-hydrogen bindings in crystal lattices (Yu, Satoshi, Masahisa, & Shigenori, 2010).

3.6. Thermal property analysis

Thermal stability, which can be analyzed using the DSC and TGA techniques, is a critical factor for determining the potential applications of chitin and its derivatives (Villetti et al., 2002). Chitin is a biopolymer that requires high thermal energy for dissociation of its crystalline structure (Bershtein, Egorov, Egorova, & Ryzhov, 1994). Polysaccharides in solid state usually have amorphous structure, which can be easily hydrated. Kittura et al. (2002) proved that hydration properties of polysaccharide macromolecules could reflect its polysaccharide composition and crystalline structure. The hydration behavior of chitin could contribute to its thermal properties and were evaluated using the TGA and DSC techniques.

TGA and corresponding DTG curves of chitin are shown in Fig. 4. Two main peaks exhibited in the DTG curves of Antarctic krill chitin, which represented two independent decomposition steps. The first step from 40 to 140 °C could be attributed to water evaporation, while the second one from 260 to 400 °C might result from the degradation of polysaccharide molecular structure, including dehydration of polysaccharide rings and polymerization and decomposition of acetylated and de-acetylated units of chitin (Paulino, Simionato, Garcia, & Nozaki, 2006). A small mass releasing occurred between 400 and 800 °C. This may be due to the formation of gaseous molecules like CO, CO_2, and H_2O according to the studies of Iqbal et al. (2011).

Temperature range values, mass loss, and activation energy (E_a) in the major decomposition stage are listed in Table 2. Antarctic krill chitin possessed significantly higher E_a value than shrimp and crab chitins in the major decomposition stage. It revealed that Antarctic krill chitin possessed better stability (Iqbal et al., 2011).

As shown in Fig. 5A, in the first heating program, the DSC curve of Antarctic krill chitin showed a sharp but wide endothermic peak in the temperature range from 52.30 to 112.38 °C. This could be due to the loss of absorbed water and hydrogen-bonded water to the polysaccharide structure as suggested in a previous study by Kacurakova, Belton, Hirsch, and Ebringerova (1998). Values for the transition temperatures and their associated enthalpies are listed in Table 3.

In the second heating program (Fig. 5B), the stepwise increase from 164.96 °C could be according to the glass transition (T_g) of Antarctic krill chitin in the thermogram. The transition was due to the local relaxation of the backbone chain of chitin (Pizzoli, Ceccorulli, & Scandola, 1991). The endothermic peak centered at 378.68 °C could be related to the decomposition of

Table 1
The *d*-spacings between atomic layers and crystalline size normal to the *h k l* plane ($D_{\perp hkl}$) of Antarctic krill, crab and shrimp chitin calculated through X-ray diffraction (XRD) analysis.

Sample	2θ (°)		*d*-Spacings (Å)		D_{hkl} (nm) *h k l*	
	0 2 0	1 1 0	0 2 0	1 1 0	0 2 0	1 1 0
Antarctic krill chitin	9.03 ± 0.02	19.17 ± 0.09	9.78 ± 0.01[a]	4.63 ± 0.02[a]	6.07 ± 0.02[a]	5.16 ± 0.02[a]
Crab chitin	9.11 ± 0.05	19.09 ± 0.08	9.70 ± 0.06[a]	4.65 ± 0.02[a]	7.67 ± 0.08[c]	6.04 ± 0.06[c]
Shrimp chitin	9.09 ± 0.05	19.08 ± 0.07	9.73 ± 0.06[a]	4.65 ± 0.02[a]	8.94 ± 0.06[b]	6.58 ± 0.02[b]

Data are presented as means ± S.E.M. ($n = 3$). Multiple comparisons were conducted using one-way ANOVA followed by Tukey's post hoc test. Means with different small letters within a column are significantly different from other group ($P < 0.05$).

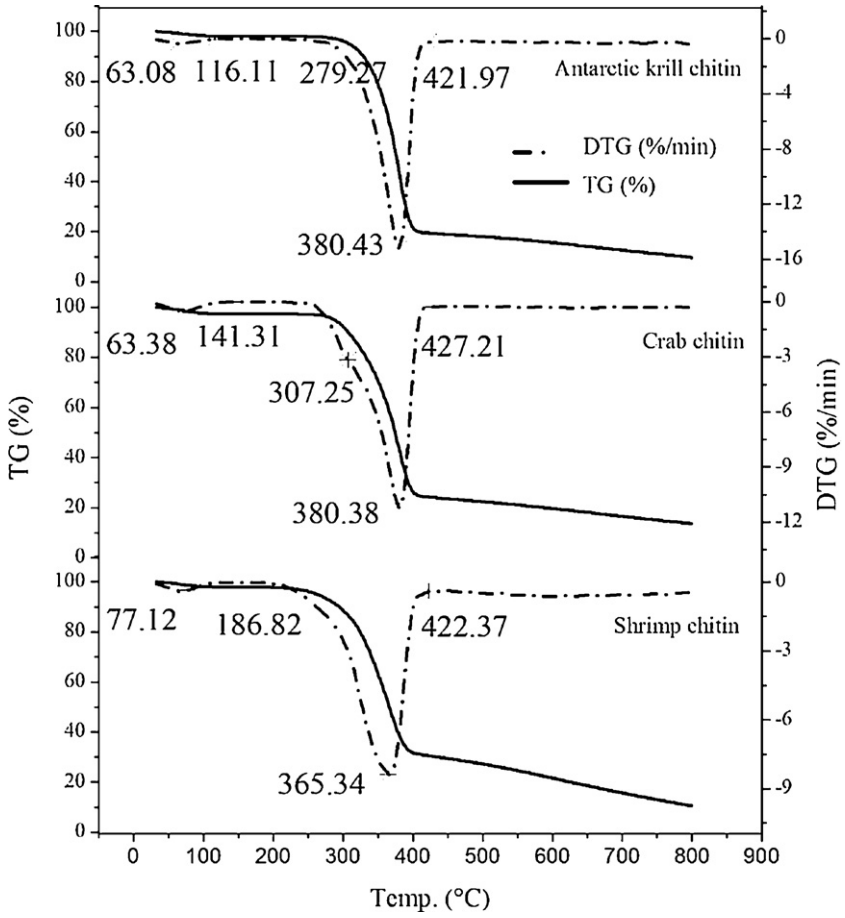

Fig. 4. Thermogravimetry (TGA) of Antarctic krill (*E. superba*) chitin, crab (*C. opilio*) chitin and shrimp (*M. affinis*) chitin.

Table 2
Values of the temperature range, mass loss, and activation energy (Ea) in the major decomposition stage of Antarctic krill chitin, shrimp and crab chitin calculating through thermogravimetry (TGA) analysis.

Sample	Temp. range (°C)	T_{max} (°C)	Mass loss (%)	E_a (kJ/mol)
Antarctic krill chitin	260–400	369.8	70.74	123.35 ± 1.20[a]
Crab chitin	260–400	380.8	63.47	99.66 ± 0.47[b]
Shrimp chitin	260–400	365.4	71.14	90.68 ± 1.10[c]

Data are presented as means ± S.E.M. ($n = 3$). Multiple comparisons were conducted using one-way ANOVA followed by Tukey's post hoc test. Means with different small letters within a column are significantly different from other group ($P < 0.05$). Temp. range, from onset temperature to completion temperature; T_{max}, the temperature for maximum reaction rate; E_a, the activation energy.

acetyl-glucosamine units (Nam, Park, Ihm, & Hudson, 2010). The exothermic peak emerging from 400 °C could result from the evaporation of volatile low molecular products that formed during depolymerization (Iqbal et al., 2011).

Table 3
Values for the transition temperatures and their associated enthalpies of the endothermic peak in the first heating run from 0 to 200 °C of Antarctic krill chitin, crab chitin and shrimp chitin calculated through differential scanning calorimetry (DSC) analysis.

Sample	Endotherm			
	T_o (°C)	T_p (°C)	T_c (°C)	ΔH (J/g)
Antarctic krill chitin	52.30	73.93	112.38	341.20 ± 2.68[a]
Crab chitin	53.08	95.87	139.01	219.40 ± 2.29[c]
Shrimp chitin	52.57	92.46	137.15	116.55 ± 2.74[b]

Data are presented as means ± S.E.M. ($n = 3$). Multiple comparisons were conducted using one-way ANOVA followed by Tukey's post hoc test. Means with different small letters within a column is significantly different from other group ($P < 0.05$). T_o, onset temperature; T_p, peak temperature; T_c, completion temperature; ΔH (J/g dry weight), peak enthalpy.

Differences of the endothermic peak temperature and area emerging in the first heating program (Fig. 5A) indicated that these chitin macromolecules differed in their water-holding capacity and strength of the water–polymer interaction. The peak-associated enthalpy of Antarctic krill chitin was the largest among the 3 types of α-chitins. According to previous studies of Iqbal et al. (2011), we found that the bound water molecules in the Antarctic krill chitin formed strong hydrogen bonds with polysaccharide chain, and were difficult to evaporate. In the second heating program, the glass transition (T_g) of Antarctic krill chitin was higher than that of reference α-chitins. This indicated good thermal stability of Antarctic krill chitin with prolonged heating.

Through the thermal property analysis, it could be concluded that Antarctic krill chitin exhibited better thermal stability than shrimp and crab chitins. The structure of chitin predominantly contributes to its thermal properties (Johannsen, Schulze, Jehnichen, Häußler, & Voit, 2011). According to FTIR results in this study, there were higher percentages of free OH groups in the structure of Antarctic krill chitin which contributed to the higher enthalpy of

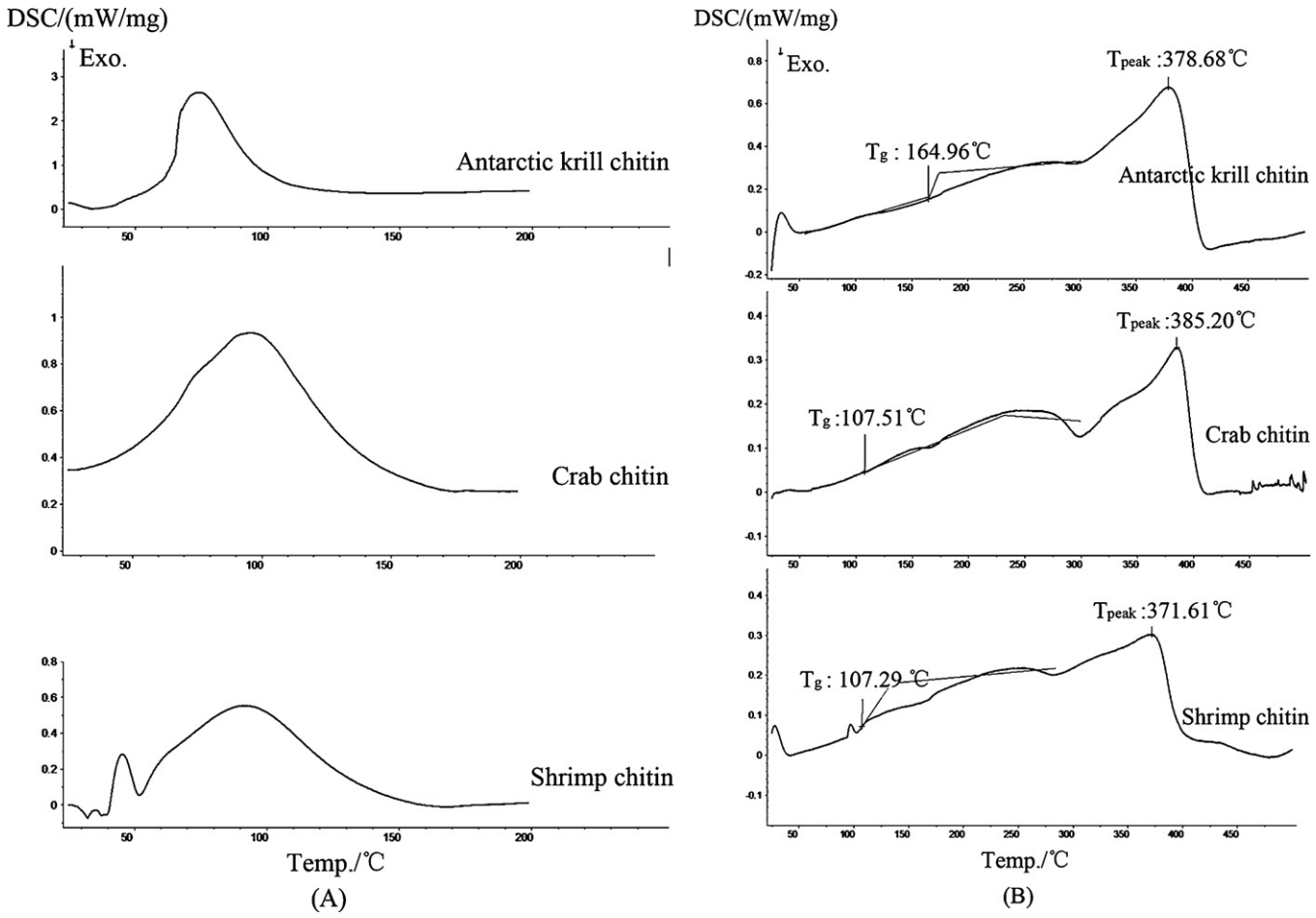

Fig. 5. Differential scanning calorimetry (DSC) of Antarctic krill (*E. superba*) chitin, crab (*C. opilio*) chitin and shrimp (*M. affinis*) chitin.

Antarctic krill chitin. Moreover, previous studies demonstrated that polymer constituted of small and medium-sized crystals possess higher thermal stability than that constituted of the large-volume crystals. The numerous small and uniform crystals in the Antarctic krill chitin might participate in maintaining the thermal stability of chitin structure. In addition, a higher percentage of acetylglucosamine units in the Antarctic krill chitin increased the thermal stability of chitin molecular chains (Kittura et al., 2002).

4. Conclusion

Antarctic krill chitin corresponded to the α-polymorph, which constituted small, stable, and uniform micro-crystals. The DD value was 11.28 ± 0.86%. The *d*-spacings of the Antarctic krill chitin were 9.78 Å and 4.63 Å at (0 2 0) and (1 1 0) planes. The crystalline sizes were 6.07 nm and 5.16 nm at (0 2 0) and (1 1 0) planes, respectively. The activation energy of the polysaccharide chain decomposition was 123.35 kJ/mol, and the glass transition (T_g) of Antarctic krill chitin was 164.96 °C.

Previous difficulties in handling *E. superba* chitin in view of the production of chitosan such as scarce solubility and colloid/aggregate formation were presumably due to the presence in chitosan of chain segments exclusively made of acetylated units that escaped deacetylation owing to poor milling and sieving (notwithstanding the similar degree of deacetylation when compared to controls). Therefore, when assessing the quality of a chitin/chitosan sample, one had better consider the heterogeneity of the deacetylation, as amply demonstrated by enzymatic studies (Terbojevich, Cosani, & Muzzarelli, 1996) and by instrumental chemical analysis (Yang, Ding, & Montgomery, 2010). The heterogeneity of the deacetylation of krill chitin would be studied in a near future.

Acknowledgements

This work was supported by National Natural Science Foundation of China (No. 31101302), National High-tech R&D Program of China (2011AA090801) and Program for Changjiang Scholars and Innovative Research Team in University.

References

AOAC. (2005). *Official methods of analysis* (18th ed.). Washington, DC: Association of Official Analytical Chemists.

Adelung, D., Buchholz, F., Culik, B., & Keck, A. (1987). Fluoride in tissues of krill *Euphausia superba* Dana and *Meganyctiphanes norvegica* M. Sars in relation to the moult cycle. *Polar Biology*, *7*, 43–51.

Al Sagheer, F. A., Al Sughayer, M. A., Muslim, S., & Elsabee, M. Z. (2009). Extraction and characterization of chitin and chitosan from marine sources in Arabian Gulf. *Carbohydrate Polymers*, *77*, 410–419.

Allowances. (1989). *Recommended dietary allowances* (10th ed.). Washington: Food and Nutrition Board, National Research Council., pp. 235–240.

Alonzo, S. H., Switzer, P. V., & Mangel, M. (2003). An ecosystem-based approach to management: Using individual behavior to predict the indirect effects of Antarctic krill fisheries on penguin forging. *Journal of Applied Ecology*, *40*, 692–702.

Atkinson, A., Siegel, V., Pakhomov, E. A., Jessopp, M. J., & Loeb, V. (2009). A re-appraisal of the total biomass and annual production of Antarctic krill. *Deep Sea Research Part I*, *56*, 727–740.

Bautista-Baños, S., Hernández-Lauzardo, A. N., Velázquez-del Valle, M. G., Hernández-López, M., Ait-Barka, E., Bosquez-Molina, E., et al. (2006). Chitosan as a potential natural compound to control pre and postharvest diseases of horticultural commodities. *Crop Protection*, *25*, 108–118.

Bershtein, V. A., Egorov, V. M., Egorova, L. M., & Ryzhov, V. A. (1994). The role of thermal analysis in revealing the common molecular nature of transitions in polymers. *Thermochimica Acta*, *238*, 41–73.
Blackwell, J. (1969). Structure of β-chitin or parallel chain systems of poly-β-(1-4)-N-acetyl-D-glucosamine. *Biopolymer*, *7*, 281–298.
Bligh, E. G., & Dyer, W. J. (1959). A rapid method of total lipid extraction and purification. *Canadian Journal of Biochemistry and Physiology*, *37*, 911–917.
Cabib, E. (1981). Chitin: Structure, metabolism and regulation of biosynthesis. *Encyclopedia of Plant Physiology*, *13B*, 395–415.
Cabib, E., Bowers, B., Sburlati, A., & Silverman, S. J. (1988). Fungal cell wall synthesis: The construction of a biological structure. *Microbiological Science*, *5*, 370–375.
Cho, Y. W., Jang, J., Park, C. R., & Ko, S. W. (2000). Preparation and solubility in acid and water of partially deacetylated chitins. *Biomacromolecules*, *1*, 609–614.
Cortizo, M. S., Berghoff, C. F., & Alessandrini, J. L. (2008). Characterization of chitin from *Illex argentinus* squid pen. *Carbohydrate Polymers*, *74*, 10–15.
Eagers, R. Y. (1969). *Toxic properties of inorganic fluoride compounds*. Amsterdam/London/New York: Elsevier., p. 152.
European Commission. (2009). *Standing committee on the food chain and animal health section general food law*. Health & Consumers Directorate-General.
Everson, I. (2000). Biological observations. In I. Everson (Ed.), *Krill: Biology, ecology and fisheries* (pp. 33–39). London: Blackwell Science.
Everson, I., & Goss, C. (1991). Krill fishing activity in the Southwest Atlantic. *Antarctic Science*, *3*, 351–358.
Farkas, V. (1990). Fungal cell walls: Their structure, biosynthesis and biotechnological aspects. *Acta Biotechnologica*, *10*, 225–238.
Fleet, G. H., & Phaff, H. J. (1981). Fungal glucans—Structure and metabolism. *Encyclopedia of Plant Physiology*, *13B*, 416–440.
Gigliotti, J. C., Davenport, M. P., Beamer, S. K., Tou, J. C., & Jaczynski, J. (2011). Extraction and characterisation of lipids from Antarctic krill (*Euphausia superba*). *Food Chemistry*, *125*, 1028–1036.
Horowitz, H. H., & Metzger, G. (1963). A new analysis of thermogravimetric traces. *Analytical Chemistry*, *35*, 1464–1471.
Hu, X. W., Du, Y. M., Tang, Y. F., Wang, Q., Feng, T., Yang, J. H., et al. (2007). Solubility and property of chitin in NaOH/urea aqueous solution. *Carbohydrate Polymers*, *70*, 451–458.
Iqbal, M. S., Akbar, J., Saghir, S., Karim, A., Koschella, A., Heinze, T., et al. (2011). Thermal studies of plant carbohydrate polymer hydrogels. *Carbohydrate Polymers*, *86*, 1775–1783.
Johannsen, M., Schulze, U., Jehnichen, D., Häußler, L., & Voit, B. (2011). Thermal properties and crystalline structure of poly(10-undecene-1-ol). *European Polymer Journal*, *47*, 1124–1134.
Kacurakova, M., Belton, P. S., Hirsch, J., & Ebringerova, A. (1998). Hydration properties of xylan-type structures: An FTIR study of xylooligosaccharides. *Journal of the Science of Food and Agriculture*, *77*, 38–44.
Kawaguchi, S., & Nicol, S. (2007). Learning about Antarctic krill from the fishery. *Antarctic Science*, *19*, 219–230.
Kittura, F. S., Harish Prashantha, K. V., Udaya Sankarb, K., & Tharanathan, R. N. (2002). Characterization of chitin, chitosan and their carboxymethyl derivatives by differential scanning calorimetry. *Carbohydrate Polymers*, *49*, 185–193.
Lavall, R. L., Assis, O. B. G., & Campana-Filho, S. P. (2007). β-Chitin from the pens of *Loligo* sp.: Extraction and characterization. *Bioresource Technology*, *98*, 2465–2472.
Liang, K., Chang, B., Tsai, G., Lee, J., & Fu, W. R. (1997). Heterogeneous N-deacetylation of chitin in alkaline solution. *Carbohydrate Research*, *303*, 327–332.
Liu, T. G., Li, B., Huang, W., Lv, B., Chen, J., & Zhang, J. X. (2009). Effects and kinetics of a novel temperature cycling treatment on the N-deacetylation of chitin in alkaline solution. *Carbohydrate Polymers*, *77*, 110–117.
Liu, T. G., Li, B., Zheng, X. D., Liang, S., Song, X., Zhu, B., et al. (2010). Effects of freezing on the condensed state structure of chitin in alkaline solution. *Carbohydrate Polymers*, *82*, 753–760.
Mangel, M., & Nicol, S. (2000). Krill and the unity of biology. *Canadian Journal of Fisheries and Aquatic Science*, *57*, 1–5.
Mauchline, J., & Fisher, L. R. (1969). The biology of Euphausiids. *Advanced Marine Biology*, *7*, 1–454.
Mayzaud, P., Albessard, E., & Cuzin-Roudy, J. (1998). Changes in lipid composition of the Antarctic krill *Euphausia superba* in the Indian sector of the Antarctic Ocean: Influence of geographical location, sexual maturity stage and distribution among organs. *Marine Ecology Progress Series*, *173*, 149–162.
Mikkelsen, A., Engelsena, B., Hansenb, H. C. B., Larsenc, O., & Skibsted, L. H. (1997). Calcium carbonate crystallization in the α-chitin matrix of the shell of pink shrimp, *Pandalus borealis*, during frozen storage. *Journal of Crystal Growth*, *177*, 125–134.
Miller, D. G. M, & Hampton, I. (1989). Biology and ecology of the Antarctic krill (*Euphausia superba* Dana): Are view. *Biomass Handbook*, *9*, 1–166.
Minke, R., & Blackwell, J. (1978). The structure of α-chitin. *Journal of Molecular Biology*, *120*, 429–433.
Morton, W. E., & Hearle, J. W. S. (1975). *Physical properties of textile fibers* (2nd ed.). Heinemann/London: The Textile Institute.
Muzzarelli, R. A. A. (1988). Carboxymethylated chitins and chitosans. *Carbohydrate Polymers*, *8*, 1–21.
Muzzarelli, R. A. A., Boudrant, J., Meyer, D., Manno, N., DeMarchis, M., & Paoletti, M. G. (2012). Current views on fungal chitin/chitosan, human chitinases, food preservation,glucans, pectins and inulin: A tribute to Henri Braconnot, precursor of the carbohydrate polymers science, on the chitin bicentennial. *Carbohydrate Polymers*, *87*, 995–1012.
Muzzarelli, R. A. A., Morganti, P., Morganti, G., Palombo, P., Palombo, M., Biagini, G., et al. (2007). Chitin nanofibrils/chitosan glycolate composites as wound medicaments. *Carbohydrate Polymers*, *70*, 274–284.
Muzzarelli, R. A. A., & Rocchetti, R. (1985). Determination of the degree of acetylation of chitosans by first derivative ultraviolet spectrophotometry. *Carbohydrate Polymers*, *5*, 461–472.
Naczk, M., Synowiecki, J., & Sikorski, Z. E. (1981). The gross chemical composition of Antarctic krill shell waste. *Food Chemistry*, *7*, 175–179.
Nam, Y. S., Park, W. H., Ihm, D., & Hudson, S. M. (2010). Effect of the degree of deacetylation on the thermal decomposition of chitin and chitosan nanofibers. *Carbohydrate Polymers*, *80*, 291–295.
Nicol, S., & Endo, Y. (1999). Krill fisheries: Development, management and ecosystem implications. *Aquatic Living Resources*, *12*, 105–120.
Paulino, A. T., Simionato, J. I., Garcia, J. C., & Nozaki, J. (2006). Characterization of chitosan and chitin produced from silkworm chrysalides. *Carbohydrate Polymers*, *64*, 98–103.
Pizzoli, M., Ceccorulli, G., & Scandola, M. (1991). Molecular motions of chitosan in the solid state. *Carbohydrate Research*, *222*, 205–213.
Rashidova, S. S., Milusheva, R., Voropaeva, Yu., Pulatova, N. L., Nikonovich, S. R., & Ruban, G. V. I. N. (2004). Isolation of chitin from a variety of raw materials, modification of the material, and interaction its derivatives with metal ions. *Chromatographia*, *59*, 783–786.
Rinaudo, M. (2006). Chitin and chitosan: Properties and applications. *Progress in Polymer Science*, *31*, 603–632.
Rudall, K. M. (1963). The chitin/protein complexes of insect cuticles. *Advances in Insect Physiology*, *1*, 257–313.
Rudall, K. M., & Kenchington, W. (1973). The chitin system. *Biology Review*, *49*, 597–602.
Saito, Y., Okano, T., Chanzy, H., & Sugiyama, J. (1995). Structural study of a chitin from the grasping spines of the arrow worm (*Sagitta* spp.). *Journal of Structural Biology*, *114*, 218–228.
Sashiwa, H., & Aiba, S. (2004). Chemistry modified chitin and chitosan as biomaterials. *Progress in Polymer Science*, *29*, 887–898.
Scherrer, P. (1918). Bestimmung der Grosse und inneren Struktur von Kolloidteilchen mittels Rontgenstrahlen. *Nachrichten Gesellschaft der Wissenschaften zu Göttingen*, *26*, 98–100.
Sikorski, P., Hori, R., & Wada, M. (2009). Revisit of α-chitin crystal structure using high resolution X-ray diffraction data. *Biomacromolecules*, *10*, 1100–1105.
Synowiecki, J., Sikorski, Z., & Naczk, M. (1982). Immobilisation of amylases on krill chitin. *Food Chemistry*, *8*, 239–246.
Terbojevich, M., Cosani, A., & Muzzarelli, R. A. A. (1996). Molecular parameters of chitosans depolymerized with the aid of papain. *Carbohydrate Polymers*, *29*, 63–68.
Villetti, M. A., Crespo, J. S., Soldi, M. S., Pires, A. T. N., Borsali, R., & Soldi, V. (2002). Thermal degradation of natural polymers. *Journal of Thermal Analysis and Calorimetry*, *67*, 295–303.
Wang, L. Z., Xue, C. H., Wang, Y. M., & Yang, B. (2011). Extraction of proteins with low fluoride level from Antarctic krill (*Euphausia superba*) and their composition analysis. *Journal of Agricultural and Food Chemistry*, *59*, 6108–6112.
Wu, T., & Zivanovic, S. (2008). Determination of the degree of acetylation (DA) of chitin and chitosan by an improved first derivative UV method. *Carbohydrate Polymers*, *73*, 248–253.
Yang, B. Y., Ding, Q., & Montgomery, R. (2010). Heterogeneous components of chitosans. *Biomacromolecules*, *11*, 3167–3171.
Yen, M. T., Yang, J. H., & Mau, J. L. (2009). Physicochemical characterization of chitin and chitosan from crab shells. *Carbohydrate Polymers*, *75*, 15–21.
Yu, O., Satoshi, K., Masahisa, W., & Shigenori, K. (2010). Crystal analysis and high-resolution imaging of microfibrillar a-chitin from *Phaeocystis*. *Journal of Structural Biology*, *171*, 111–116.